Electronic Supplementary Material (ESI) for Chemical Science.

Supporting Information

Jie Tang [a][+], Yang Yang [a][+], Jingjing Qu[a], Wenhuang Ban[a], Hao Song[a], Zhengying Gu[b], Yannan Yang[a], Larry Cai[a], Shevanuja Theivendran[a], Yue Wang[a], Min Zhang[b], and Chengzhong Yu[a,b]*

[a] Australian Institute for Bioengineering and Nanotechnology, the University of Queensland, St Lucia, Brisbane, QLD 4072, Australia. *E-mail: c.yu@uq.edu.au

[b] School of Chemistry and Molecular Engineering East China Normal University Shanghai 200241, China. * E-mail: czyu@chem.ecnu.edu.cn

[+] These authors contributed equally to this work.

Methods

Chemicals and biological reagents: Cetyltrimethylammonium bromide (CTAB), tetraethyl orthosilicate (TEOS), triethanolamine (TEA), ethanol, sodium aluminate ($Na_2Al_2O_4$), acetic acid (HAc), sodium acetate (NaAc), aluminum chloride hexahydrate and ovalbumin (OVA) were purchased from Sigma-Aldrich. Alhydrogel® adjuvant 2% (Alhydrogel) was purchased from InvivoGen. Roswell Park Memorial Institute (RPMI)1640 Medium and Dulbecco's modified eagle medium (DMEM) were purchased from Life Technologies. The Magic Red Cathepsin B kit and the FAMFLICA® Caspase-1 Assay kit were purchased from ImmunoChemistry Technologies. The ELISA Kits for testing the cytokeins, including IL-1beta, IFN-garma, IL-18 and TNF-α were purchased from Abcam. Antibodies for immunohistochemistry staining against cleaved caspase 1 and CD11c were purchased from Abcam. The antibodies used to stain the cells, including anti-mouse MHC I, CD40, CD80, CD86, CD3, CD4, CD8α and IFN-γ were perchased from BioLegend. DC 2.4 were perchased from American Type Culture Collection (ATCC).

Synthesis of dendritic mesoprous silica nanoparticles (DMSN): DMSN were synthesized via a one-pot synthesis using CTAB and NaSal as structure directing agents, TEOS as a silica source and TEA as a catalyst. In a typical synthesis, 0.68 g of TEA were added to 250 mL of water and stirred gently at 80 °C in an oil bath under stirring for 0.5 h. Afterwards, 3.80 g of CTAB and 1.68 g of NaSal were added to the above solution, the mixture solution was stirred for another 1 h. Then, 40 mL of TEOS and 5 mL of ethanol were mixed before added to the above solution under stirring (~ 300 rpm). After reaction for another 3 h, the products were collected by high-speed centrifugation (4700 rpm at RT, 10 min) and washed three times by distilled water and

ethanol to remove the residual reactants. Finally, the collected products were calcined at 550 °C for 6 h to remove the structure directing agents.

Synthesis of Na-^{IV}Al-DMSN: Typically, 800 mg of calcined DMSN prepared in the previous step were dispersed in 200 mL deionized water containing 218 mg of sodium aluminate. The mixture was subject to ultrasonic treatment in water bath for 30 min at room temperature. Then, the mixture solution was thoroughly stirred for another 3 h at 60 °C. Afterwards, Na-^{IV}Al-DMSN were obtained through centrifugation at 4700 rpm for 10 min, washed three times by distilled water to remove the residual reactants, and dried under vacuum at 80 °C for 12 h.

Synthesis of H-^{IV}Al-DMSN**:** 800 mg of DMSN were dispersed in 100 mL of NaAc-HAc buffer solution at pH of 3.8, followed by ultrasonic treatment for 30 min. Then, 20 mL of aluminum chloride hexahydrate solution with Al concentration of 21 mM were added dropwise under stirring, and the mixture solution was stirred thoroughly for 3 h at 60 °C. The products were collected by high-speed centrifugation (4700 rpm at RT, 10 min) and washed three times by distilled water to remove the residual reactants. The procedure was repeated three thimes to increase the amount of grafted Al on DMSN. Finally, the collected products were dried under vacuum conditions at 80 °C for 12 h.

Material characterization**:** Transmission electron microscopy (TEM) images were acquired on a JEOL-1010 microscope. Scanning electron microscopy (SEM) measurements were taken by a JEOL-7800F field emission electron microscope operated at 0.5 kV. For TEM measurements, the samples were prepared by soaking the powder samples in ethanol with ultrasonication, and then they were dispersed on on a copper grid. Micromeritics Tristar 3020 system was used to characterize the porosity. The samples were pre-treated under vacuum line at 200 °C overnight. The Brunauer-Emmett–Teller (BET) method was utilized to calculate the specific surface areas

by using the adsorption data at a relative pressure (P/P_0) range of 0.05-0.35. Barrett-Joyner-Halanda (BJH) method was utilized to obtain the pore-size distribution curves of the samples from the adsorption branches of the isotherms. The total pore volume was calculated from the amount adsorbed at a maximum relative pressure (P/P_0) of 0.99. The X-ray diffraction (XRD) pattern was recorded on a Rigaku Miniflex X-ray diffractometer with Ni-filtered Cu Kα radiation (λ=1.5406 Å). X-ray photoelectron spectroscopy (XPS) profiles were acquired using a Kratos Axis ULTRA. The atomic ratios were calculated using the CasaXPS version 2.3.14 software and a Shirley baseline with the Kratos library relative sensitivity factors (RSFs). Peak fitting of the high-resolution data was also carried out using the same software. The attenuated total reflection - Fourier transform infrared (ATR-FTIR) spectra were collected with Thermo Nicolet Nexus 67000 FTIR spectrometer equipped with Diamond ATR Crystal. For each spectrum, 120 scans were collected at a resolution of 4 cm^{-1} over the range 500-4000 cm^{-1}. Dynamic light scattering (DLS) results and zeta potential values in aqueous solution were collected at 25 °C using a Zetasizer Nano-ZS from Malvern Instruments. ^{1}H magic-angle spinning nuclear magnetic resonance (MAS NMR) and ^{27}Al MAS NMR spectra were measured by a solid state Bruker Advance III spectrometer.

Release profiles of Na^+ ions: The pH dependent sodium ions release profiles from Na-^{IV}Al-DMSN were studied by varying the pH of the PBS buffer from 4.5-7.4. 1 mg Na-^{IV}Al-DMSN was dispersed in sodium free PBS at differ:ent pH values. After 2 h incubation, samples were shake and centrifuged (13000 rpm at 4 °C, 10 min) to remove nanoparticles. The quantification of released Na^+ in buffer samples was conducted by inductively coupled plasma-optical emission spectrometry (ICP-OES).

Buffering capacity test: The buffering capacity of alhydrogel, DMSN, Na-^{IV}Al-DMSN and H-^{IV}Al-DMSN were determined by measuring the pH changes after incubation in pH 5 PBS buffer. Briefly, each formulation was dispersed in PBS solution (2 mg/mL) at pH 5 and incubated for 24 h. Then, the pH values were recorded using a pH meter.

Cell Viability Test: The cell viability was measured using tetrazolium dye (MTT) colorimetric assay. Briefly, DC 2.4, RAW264.7 cells and CT26 cells were seeded in 96-well plates at a density of 3×10^3 cells per well overnight. Next day, cells were treated with Na-^{IV}Al-DMSN at various concentrations. After 24 h incubation, the cell viability was determined. All experiments were performed in triplicate.

ICP measurement for intracellular ions: Determination of intracellular K^+, Na^+ concentration through ICP-OES. Cells treated with various nanoparticles for 6h and 16h were washed with Na^+-free HEPES for tree times to remove the excess particles and were then digested by boiling in ultrapure HNO_3 for 1 h before sending off for ICP analysis.

Intracellular ROS detection by using flow cytometry: Intracellular reactive oxygen species (ROS) level was investigated by using 2′,7′- dichlorofluorescein diacetate (DCF-DA) as a fluorescent probe. Briefly, DC 2.4 cells were seeded in 12-well plates at a density of 1.5×10^5 per well and incubated in complete DMEM medium at 37 °C overnight. Afterwards, the culture medium was removed and washed twice with PBS and 50 μg/mL nanoparticles were incubated with the cells in fresh media for 6 h. Then ROS probe was added with the concentration of 100 μM in PBS for 15 min in incubator. Cells were washed with PBS and examined under Beckman Coulter CytoFLEX system.

Mitochondrial Superoxide Assay: DC 2.4 cells were seeded at 1.5×10^5 cells/mL in 12-well glass-bottom plates overnight in incubator and then exposed to 5 μg/mL Na-^{IV}Al-DMSNs/OVA

complex for up to 6h. H-^{IV}Al-DMSN, Alhydrogel, DMSN loaded with OVA were used as controls. Mitochondrial superoxide production in the cells was measured using MitoSOX fluorescence probe in Hank's Buffered Salt Solution (HBSS) containing calcium and magnesium, according to the manufacturer's protocol. MitoSOX was added to a final concentration of 5 μM in HBSS. Cells were allowed to load MitoSOX for 30 min and the cells were washed twice with HBSS. A confocal fluorescence microscopy (SP8, Leica) as used for taking fluorescent pictures. The intensity was subsequently analyzed by using NIH ImageJ software.

Cathepsin B release and caspase-1 activation test using confocal microscopy: DC 2.4 or RAW264.7 cells were seeded in 12-well culture plates at a density of 1.5×10^5 cells per well. The materials treated cells were stained with either Magic Red or FAM-FLICA® Caspase-1 (FAM-YVAD-FMK) at 37 °C following the manufacture's protocols. The cells were then fixed in a 4% paraformaldehyde PBS solution and mounted with VECTASHIELD anti-fade mounting medium containing DAPI (H-1200) (Vector Laboratories, US). Confocal images were taken on a Leica SP8 Confocal Microscope. The intensity of Magic Red was subsequently analyzed by using NIH ImageJ software.

Caspases-1 activation measured by flow cytometry: For caspase-1 analysis, DC 2.4 cells were seeded at 1.5×10^5 cells/well in 12-well plates overnight and then incubated with varies nanoparticles for 6 h. The FAM-FLICA® Caspase-1 kit (FAM-YVAD-FMK) was used for cellular staining following the manufacturer's protocol. All the cells were collected and analyzed on a Beckman Coulter CytoFLEX system using the FITC channel. The results were analyzed with FlowJo 10.0 for caspase-1 activation.

Pyroptosis assay using flow cytometry: Pyroptosis was determined by using a FAM-FLICA Caspase-1 Detection kit (ImmunoChemistry, USA). Briefly, after treatment with different

nanoparticles/OVA complexex for 24 h, DC2.4 cells were harvested to stain with FAM-FLICA® Caspase-1 green dye and PI red dye. Then a flow cytometer (Beckman Coulter CytoFLEX) was employed to analyze the samples, and PI red and FAM-FLICA green double stained cells were defined as pyroptosis.

In vitro cytokine secretion measurement: The DC 2.4 were seeded in 12 well plates at a density of 1.5×10^5 cells/well. For measuring IL-18, IFN-gama, IL-1β and TNF-α, the cells were pre-treated with lipopolysaccharide (LPS, 25 ng/mL) for 3 h before exposure to OVA loaded nanoparticles (5 μg/mL) for 12 h. Then, the supernatant was collected and analyzed with ELISA kits according to the manufacture protocols.

In vitro MHC-I cross presentation: For the cross-presentation assay, DC2.4 cells were seeded at 1.5×10^5 per well cells/well in 12-well plates and incubate overnight. PBS, OVA, DMSN/OVA, Alhydrogel/OVA, H-^{IV}Al-DMSN/OVA and Na-^{IV}Al-DMSN were added to the wells and incubated for 24 h. After incubation, cells were harvested and stained with PE-labeled SIINFEKL/H2-K^b antibody (Clone 25-D1.16) bound to the $OVA_{257–264}$ peptide. Expression patterns of H-$2K^b$-$OVA_{257–264}$ complex on DCs were assessed by flow cytometer (Beckman Coulter CytoFLEX). Each experiment was run in triplicate.

In vitro maturation of APCs: DC 2.4 cells were seeded at 1.5×10^5 per well cells/well in 12-well plates and incubate overnight. PBS, OVA, DMSN/OVA, Alhydrogel/OVA, H-^{IV}Al-DMSN/OVA and Na-^{IV}Al-DMSN were added to the wells and incubated for 24 h. The adherent cells were scraped from the plate and incubated with Fc-block for 20 min at 4 °C, centrifuged and resuspended in a buffer containing CD40 (clone FGK45), CD80 (clone 16-10A1), CD86 (clone GL-1) antibodies (BioLegend) for 30 min at 4 °C. The cells were then centrifuged and

resuspended in 0.5 mL of cell staining buffer and analyzed using flow cytometer (Beckman Coulter CytoFLEX).

Animals: All animal work was performed in accordance with Animal Ethics (AIBN/489/16) approved by the University of Queensland Institutional Animal Care and Use Committee. Female BALB/c or C57BL/6 (5~6 weeks) mice were kept in filter-topped cages with standard rodent chow and water available ad libitum in a 12 h light/dark cycle.

Immunization of mice and detection of OVA-specific antibody production: Mice were weighed and randomly divided into five groups (5 mice per group). Pre-immunization blood samples were collected by retro-orbital bleeds. The injection doses administered were OVA (50 μg) in 250 μg DMSN, Alhydrogel, H-^{IV}Al-DMSN and Na-^{IV}Al-DMSN. Doses prepared in saline were administered by subcutaneous injection at the tail base using a sterile needle (Terumo, Tokyo, Japan). Three injections were administered at three-week intervals and mice were euthanized 14 d after the final immunization. The production of anti-OVA IgG1, IgG2a, total IgG antibodies in plasma on day 42 (14 days after the third injection) were detected using ELISA.

Isolation of Murine Splenocytes and ELISA Assays: Spleen cells were removed following euthanasia and placed into ice cold complete meidum (5 mL). Spleens were gently disrupted and passed through a nylon mesh (100 μm, Becton Dickinson, Franklin Lakes, NJ) using a syringe plunger. Cells were washed with the meidum (5 mL) and centrifuged (1300 rpm, 5 min,) and then resuspended in lysis buffer (NH_4Cl, 0.15 M), $KHCO_3$ (10×10^{-3} M), Na_2-EDTA (0.1×10^{-3} M, 1 mL) for 5 min at room temperature. Repeat wash steps twice with the medium each time and cell pellets were resuspended in the medium (2 mL). Cells from each mouse spleen were seeded at 1.5×10^5 cells per well in triplicate into 96 well plate. Cells were incubated in complete medium at 37 °C and 5% CO_2 for 48 h in the presence or absence of 1μg synthetic $OVA_{257-264}$

peptide. The supernatants were then collected and the IFN-γ and IL-1β concentrations were measured using ELISA Assay according to the manufacturer protocols.

***Preparation of Tumor Lysate*:** CT26 cells lysates were performed using 3 x 10^4 tumor cells killed by 5 min heating at 42°C followed by 1 cycle of freezing/thawing in liquid nitrogen. Larger particles and cell debris were removed by centrifugation (500 g for 10 min at 4 °C). After passed through a 0.2 μm filter, supernatants were lyophilized and store at 4 °C until use.

Tumor challenge and evaluation of anti-tumor immunity: Female Balb/c mice (5-6 weeks old) were weighed and randomly divided into five groups (5 mice per group), and subcutaneously injected with free CT26 cell lysates, CT26 cell lysates loaded DMSN, Alhydrogel, H-^{IV}Al-DMSN and Na-^{IV}Al-DMSN into the left flank for three times at two-week interval. Seven days after the third immunization, the mice were challenged into the right flank with 5 x 10^5 live CT26 cells. Tumor growth was then monitored every other day. The tumor volume was calculated according to the formula (length)×(width)^2/2. Animals were sacrificed on Day 16 after the challenge with CT26 tumor cells. On Day 16, after euthanizing the animals, the tumors were collected, weighed, washed with PBS and fixed in the 10% formalin for H&E and TUNEL staining. Major organs, including spleens, liver, lung, heart and kidneys were also harvested, and fixed in 4% paraformaldehyde, sectioned, and stained with H&E for evaluating the toxicity of the nanoformulation. Paraffin-embedded sections of spleen tissues were deparaffinized and hydrated followed by antigen retrieval for immunohistochemistry staining against cleaved caspase-1 (clone D57A2). Mouse sera samples was collected for cytokines IL-1β and IL-18 determination with the ELISA kit. Splenocytes and single cells from tumor tissues were isolated to conduct flow cytometry study.

Then, the cells were incubated with Fc Block (TruStain fcX™ (anti-mouse CD16/32) Antibody, BioLegend) for 10 min, followed by surface staining with Brilliant Violet 421 anti-mouse CD3 (17A2, BioLegend), PE anti-mouse CD4 (GK1.5, BioLegend), PerCP/Cyanine5.5 anti-mouse CD8a Recombinant Antibody (QA17A07, eBioscience), APC/Cyanine7 anti-mouse CD49b ($DX5^+$, BioLegend), FITC anti-mouse CD11c Antibody (N418, BioLegend), PE anti-mouse CD80 Antibody (16-10A1, Biolegend), APC anti-mouse CD86 Antibody (GL-1, Biolegend), FITC anti-mouse/human CD44 Antibody (QA19A43, Biolegend), APC anti-mouse CD62L Antibody (MEL-14, Biolegend), and FITC anti-mouse IFN-γ Antibody (XMG1.2, Biolegend) at 4°C for 30 min in dark.

Multiparameter staining was used to identify the following populations of interest: (a) $CD8^+$ T cells ($CD3^+CD8^+$), (b) $CD4^+$ T cells ($CD3^+CD4^+$), (c) NK cells ($DX5^+CD3^-$), (d) $CD8^+IFN\gamma^+$ T cells ($CD3^+CD8^+IFN\gamma^+$), (e) $CD4^+IFN\gamma^+$ T cells ($CD3^+CD4^+IFN\gamma^+$), (f) $IFN\gamma^+$ NK cells ($DX5^+CD3^-IFN\gamma^+$), (g) $CD80^+CD86^+$ DCs ($CD11c^+CD80^+CD86^+$), (h) effector memory T cells ($CD44^+CD62L^-CD8^+$). For intracellular IFN-γ staining, cells were further fixed and permeabilized using Fixation/Permeabilization Solution Kit (BD Pharmingen). Cells were then washed and fixed by 4% PFA for flow cytometry analysis using LSR II flow cytometer. The data were processed by FlowJo 10.0. Doublets were excluded based on forward and side scatter.

Antitumor activity test in therapeutic colon cancer models: 5 x 10^5 live CT26 cells were subcutaneously implanted into the right flank of mice (5 mice per group) on day 0, and the tumors were allowed to grow for 7 d to a size of about 30-40 mm^3. The first therapeutic injection was administered on the left flank on day 7, free CT26 cell lysates, CT26 cell lysates loaded DMSN, Alhydrogel, H-^{IV}Al-DMSN and Na-^{IV}Al-DMSN into the left flank. The second injection was performed on day 14 with the same doses of CT26 cell lysates. Tumor growth was then

monitored every other day. The tumor volume was calculated according to the formula (length)×(width)^2/2. Mice were euthanized when tumor length exceeded 2 cm or when mice showed signs of pain or distress such as immobility, a hunched posture or a lack of eating. Splenocytes and single cells from tumor tissues were isolated to conduct flow cytometry study.

***Statistical Analyses*:** Experiments were assessed for significance using one-way ANOVA, followed by the Bonferroni post-test, unless noted otherwise. All statistical analyses were done with GraphPad Prism 9.0 (GraphPad Software). A significance threshold of $P < 0.05$ was applied to all comparisons.

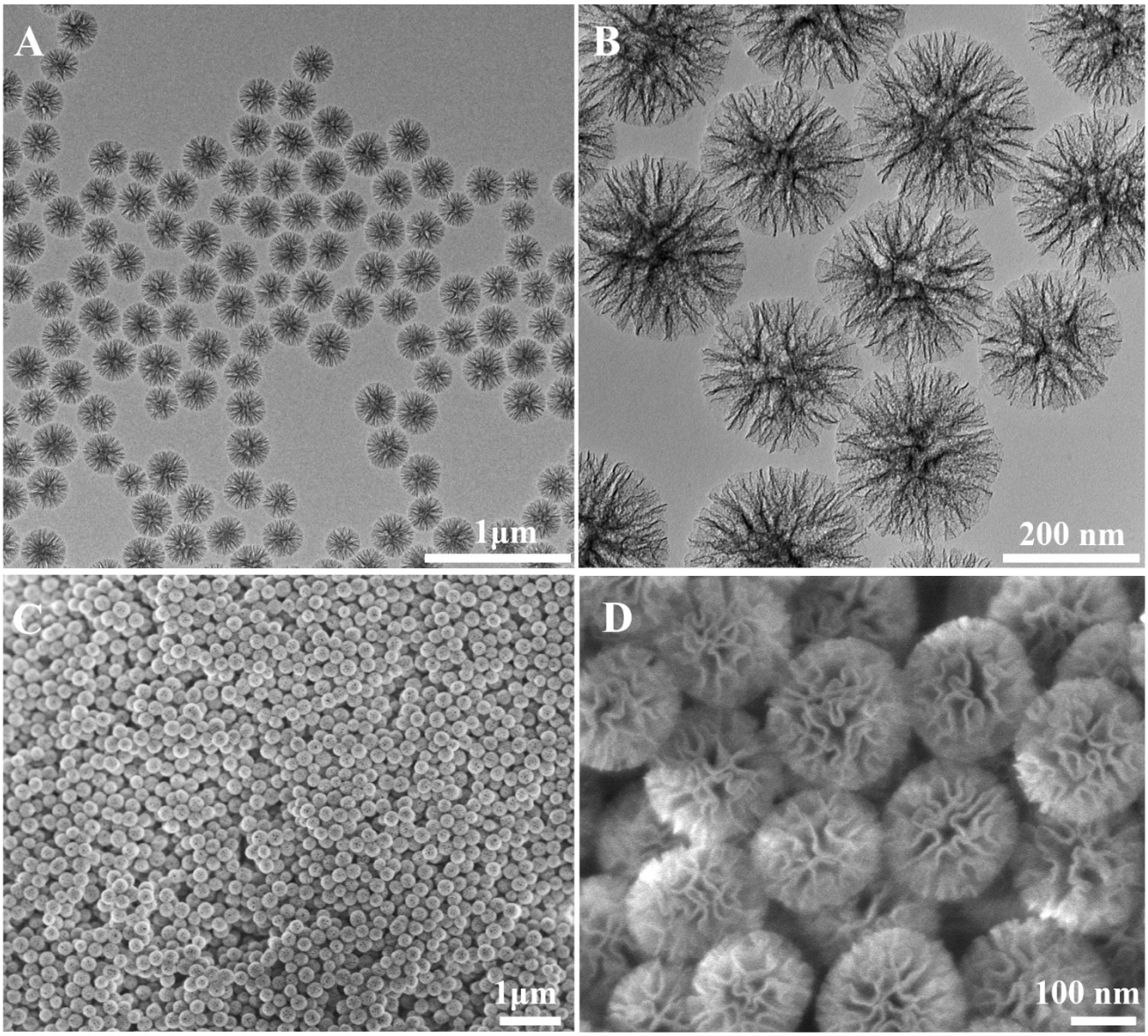

Figure S1. TEM (A and B) and SEM images (C and D) of calcined DMSN.

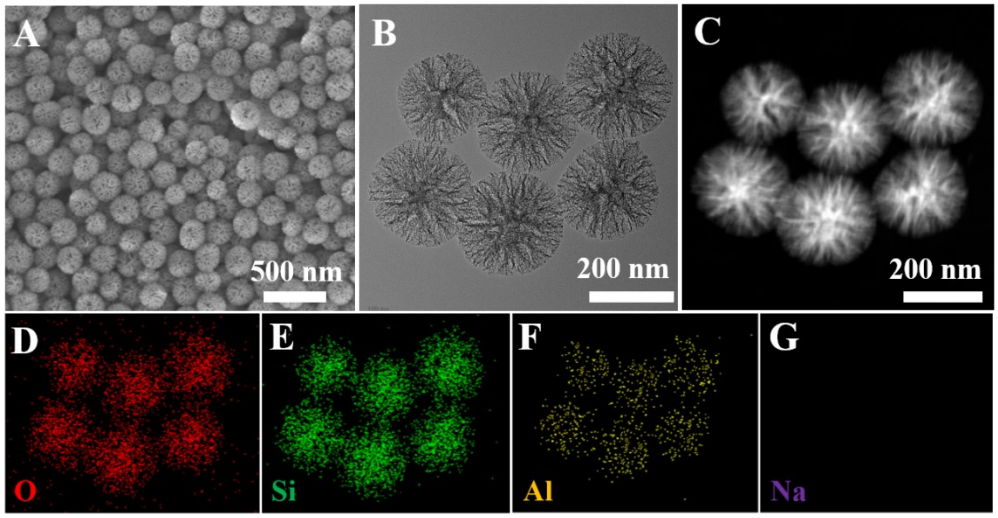

Figure S2. SEM (A), TEM (B), Dark-field STEM images (C) and EDS mapping (O, Si, Al and Na) images of H-^{IV}Al-DMSN

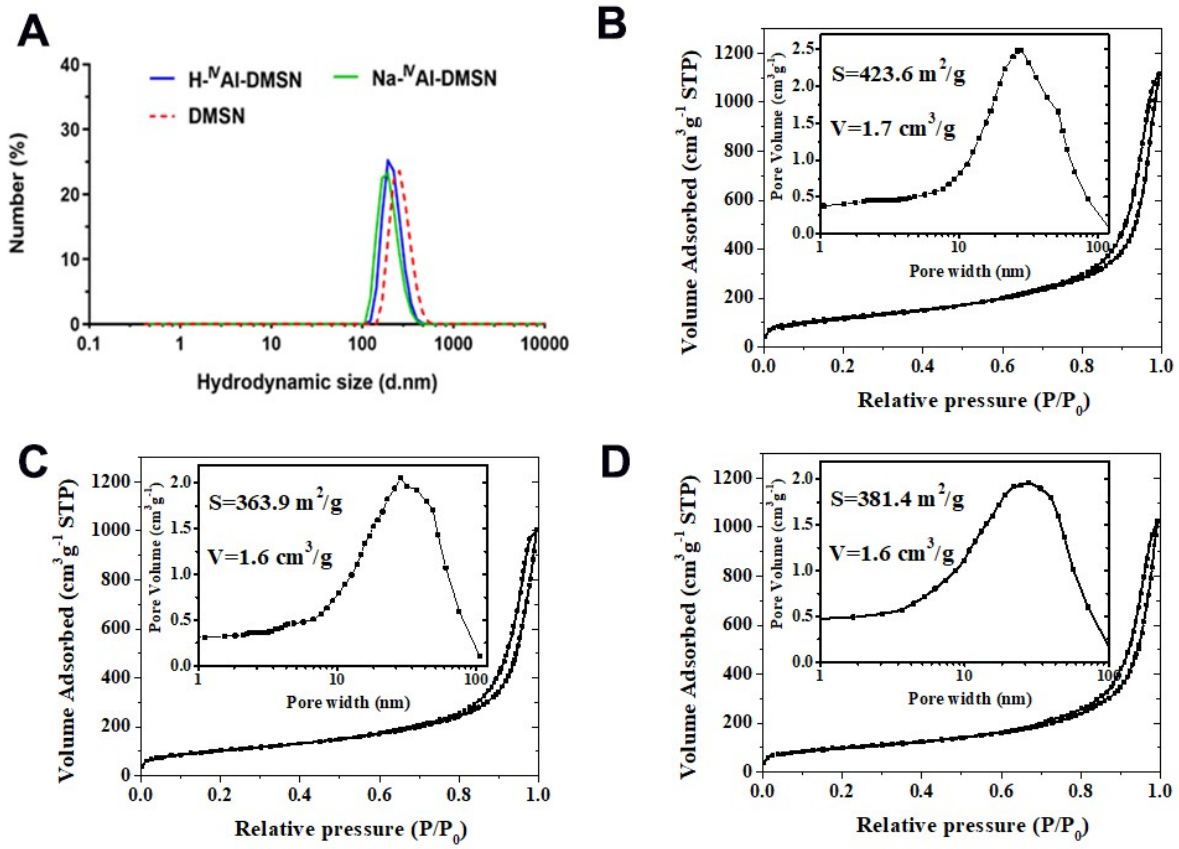

Figure S3. (A) Dynamic light scattering (DLS) analysis of DMSN, Na-^{IV}Al-DMSN and H-^{IV}Al-DMSN. The nitrogen adsorption-desorption results of (B) DMSN, (C) Na-^{IV}Al-DMSN and (D) H-^{IV}Al-DMSN.

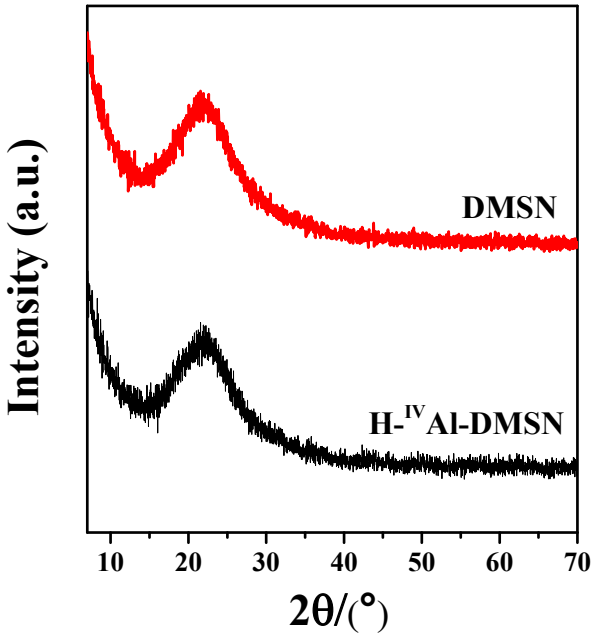

Figure S4. XRD results of DMSN and H-^{IV}Al-DMSN.

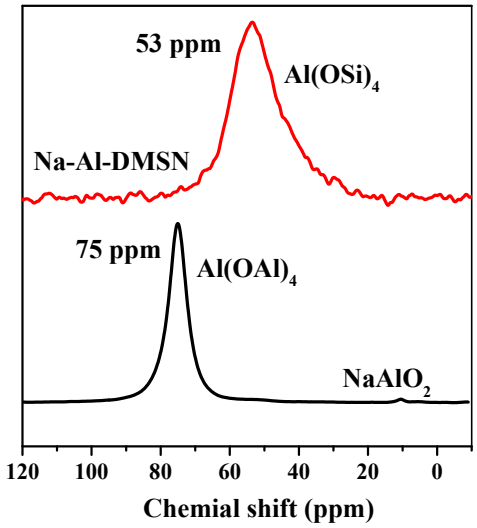

Figure S5. ^{27}Al MAS NMR results of $NaAlO_2$ and Na-^{IV}Al-DMSN.

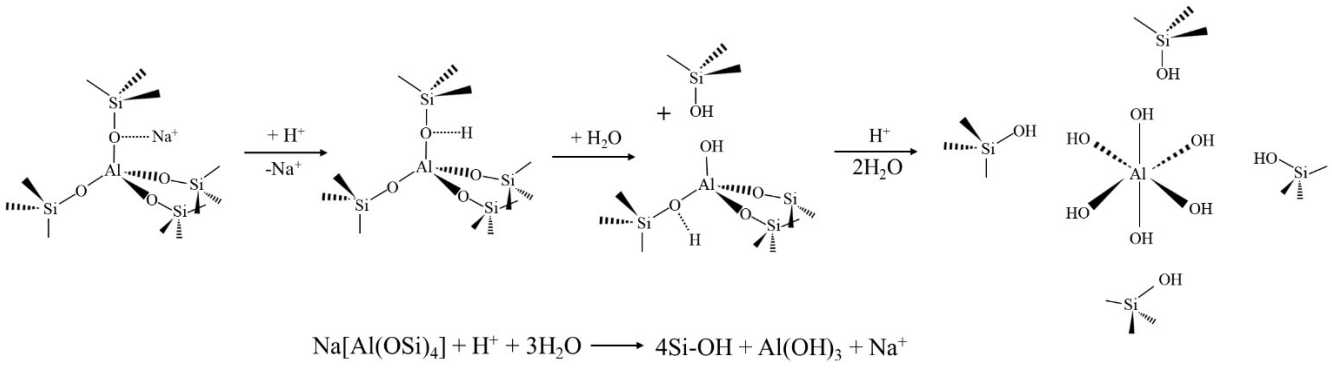

Figure S6. Proposed mechanism of the proton exchange and hydrolyzation of Na-^{IV}Al-DMSN in acidic solution.

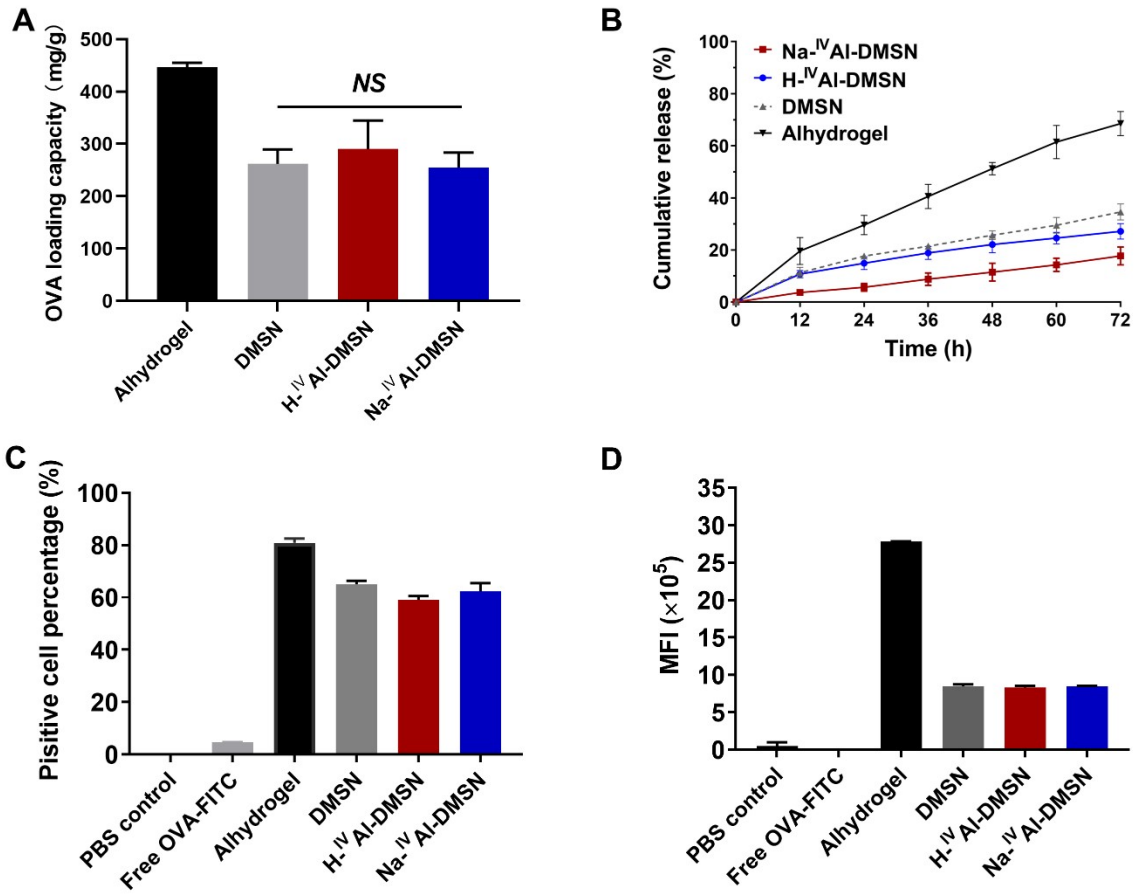

Figure S7. (A) OVA loading capacity and (B) time-dependant OVA release profiles of DMSN, Na-^{IV}Al-DMSN, H-^{IV}Al-DMSN and Alhydrogel. The Flow cytometry (C and D) were used to measure the model antigen FITC-OVA delivery efficacy in dendritic cells at nanoparticle concentrations of 50 μg·mL^{-1} and OVA concentration of 10 μg·mL^{-1}. OVA-FITC positive cell percentages (C) and mean fluoresce intensity (MFI) (D) were tested in different groups in triplicates. *p<0.05, **p<0.01, ***p<0.001.

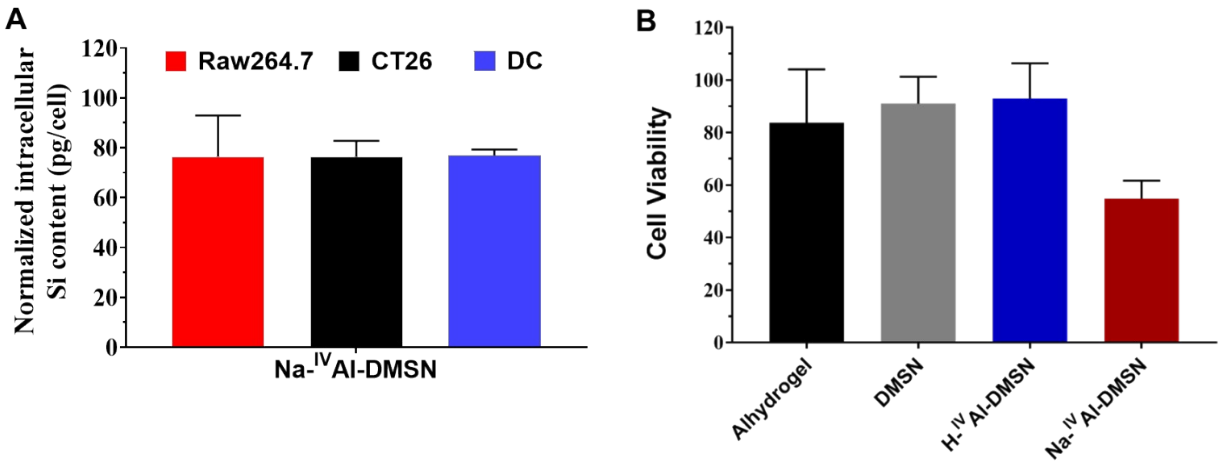

Figure S8. (A) Cell line-dependent cellular uptake of Na-^{IV}Al-DMSN nanoparticles at 24 h time point, verified by measuring Si content in cells via ICP-OES test. (B) Nano-formulations-dependent cytotoxicity (50 μg/mL) in DC 2.4 cells measured by MTT assays.

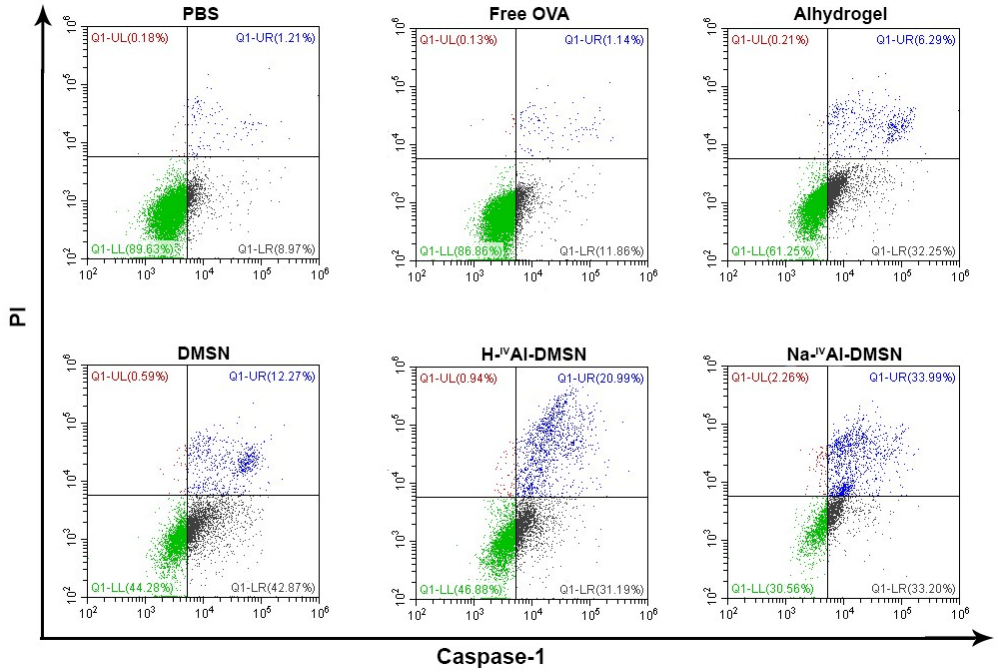

Figure S9. FAM-FLICA Caspase-1 probe/PI co-staining and flow cytometric determination of pyroptosis in DC2.4 cells. Percentage denotes proportion of apoptotic cells in right lower quadrant and right upper quadrant.

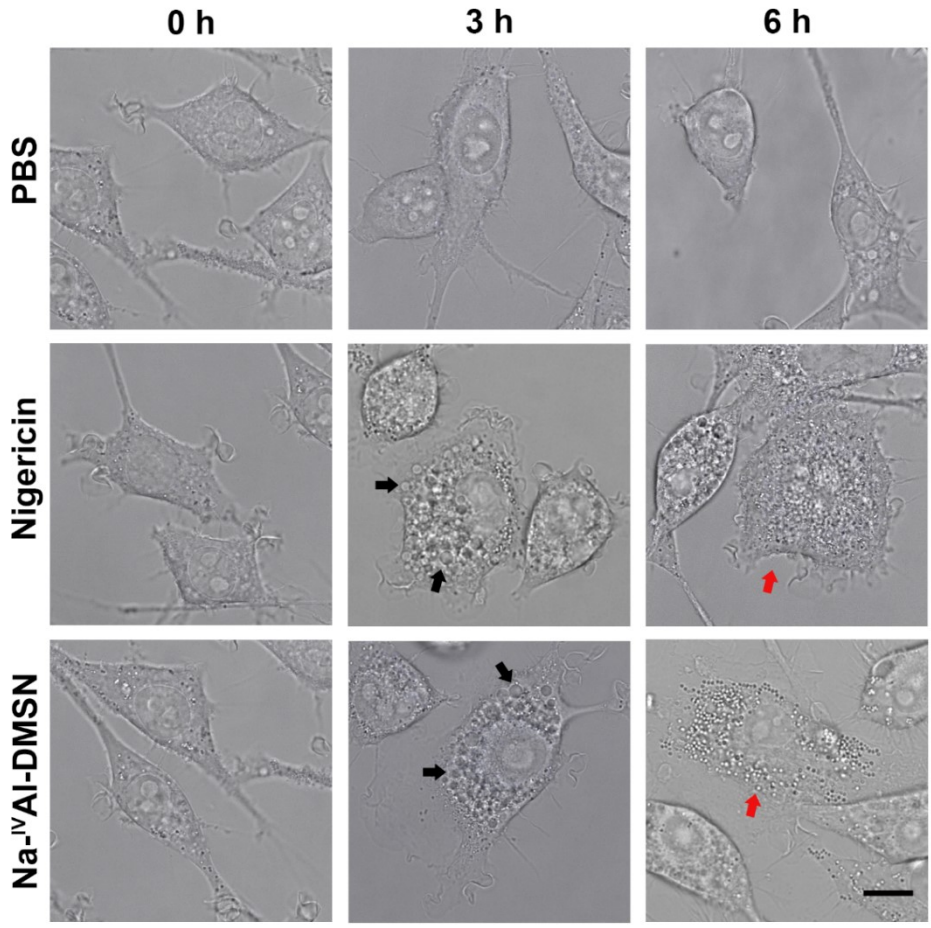

Figure S10. Representative images of DC2.4 cells treated with Na-^{IV}Al-DMSN at 0, 3 and 6 h incubation, PBS were used as negative controls, while nigericin (10 μM) was used as a positive control. The black arrow indicates pyroptotic body formation and the red arrow points to cell flattening of pyroptotic cells. Scale bar, 10 μm.

Nigericin, a potent potassium ionophore which is reported to active caspase-1-mediated pyroptosis in LPS-primed macrophages, was used as a positive control. As shown in Figure S10, pyroptotic bodies were formed after 3 h both in Na-^{IV}Al-DMSNs and Nigericin groups. After 6 h, cells treated with Na-^{IV}Al-DMSNs looked like fried egg with the cell's nucleus located in the center, and cells remain tightly attached to culture slides with flattened cytoplasms. These observations reveal a clear morphology change in cells during pyroptosis, which is associated with pyroptotic body formation and cell flattening (*Cell research* 26.9 (2016): 1007-1020; *Cell research* 28.1 (2018): 9-21.). Propidium iodide (PI, a membrane-impermeant nucleic acid intercalator) and FAM-FLICA Caspase-1 probe co-staining was conducted in DC2.4 cells after nanoparticle incubation as a measure of plasma membrane pore formation (Figure S9 in the Supporting Information). Na-^{IV}Al-DMSNs treated DCs showed significantly higher PI uptake than control groups, indicating plasma membrane pore formation.

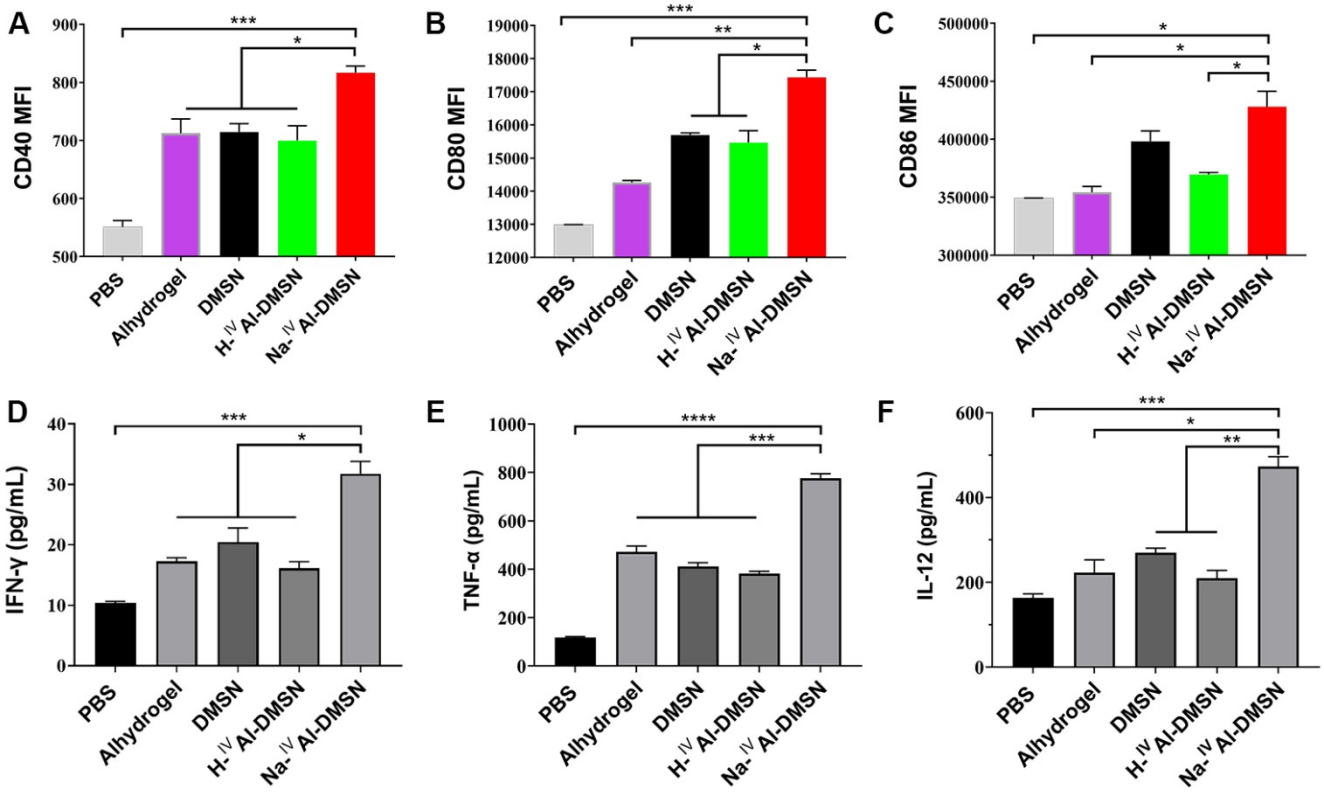

Figure S11. Na-^{IV}Al-DMSN enhance DC maturation in vitro. A, Upregulation of the activation markers CD40, CD80 and CD86 on DCs. DC2.4 cells were incubated with Alhydrogel, DMSN, H-^{IV}Al-DMSN and Na-^{IV}Al-DMSN for 12 h. The expression of the (A) CD40, (B) CD80 and (C) CD86 markers were analysed by flow cytometry. MFI, mean fluorescence intensity. (D) IFN-gamma, (E) TNF-α and (F) IL-12 in DC culture supernatants incubated with various fomulations for 24 h were analyzed using ELISA kit.

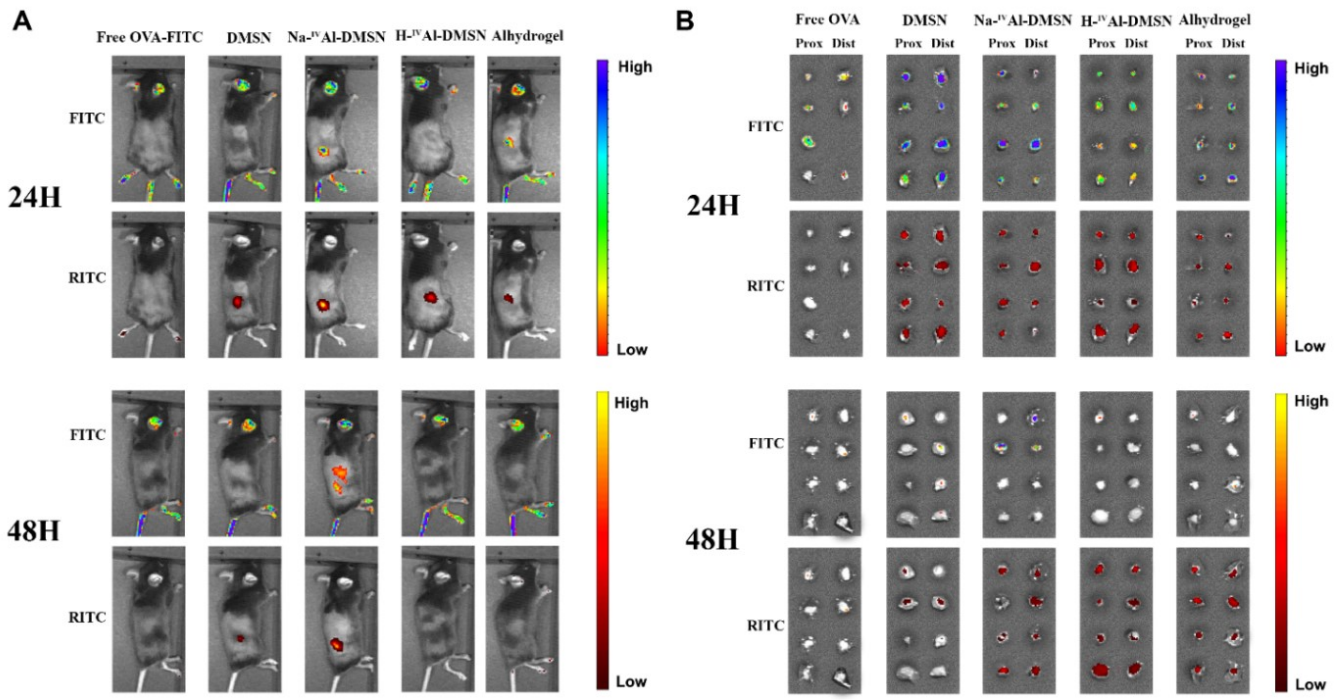

Figure S12. Antigen loaded NPs migration and accumulation in lymph nodes (RITC labeled nanoparticles loaded with FITC-OVA). C57BL/6 mice were subcutaneously injected with soluble OVA-FITC (50 mg/mouse), OVA-FITC loaded with Alhydrogel, OVA-FITC loaded DMSNs, OVA-FITC loaded Na-^{IV}Al-DMSNs, and OVA-FITC loaded H-^{IV}Al-DMSNs (250 mg particles/mouse, containing 50 mg OVA-FITC/mouse). (A) Imaging of the mouse injected with RITC labelled nanoparticles/OVA-FITC at different time points. (B) Imaging of proximal lymph nodes (left) and distal lymph nodes (right) at 24 h time point and 48 h time point.

Lymph nodes (LNs) are peripheral lymphoid organs where activated APCs can interact with T cells and B cells to initiate the adaptive immune response. To investigate the antigen release behavior at injection site and assess whether the OVA loaded Na-^{IV}Al-DMSN could efficiently migrate to LNs, the in vivo premature leakage of antigen and antigen loaded NPs migration were investigated. For the *in vivo* tracking, particles were labeled with rhodamine isothiocyanate (RITC, red fluorescence) and loaded with FITC-OVA. C57BL/6 mice were subcutaneously injected with soluble OVA-FITC (50 mg/mouse), OVA-FITC loaded with Alhydrogel, OVA-FITC loaded DMSN, OVA-FITC loaded Na-^{IV}Al-DMSN, and OVA-FITC loaded H-^{IV}Al-DMSN (250 mg particles/mouse, containing 50 mg OVA-FITC/mouse). The *in vivo* distribution and antigen accumulation at lymph

nodes were monitored by detecting fluorescence at various time points post-injection using a Xenogen *in vivo* imaging system.

As shown in Figure S12A, the FITC signal in the injection site was not detected after 24 h post injection in free OVA-FITC group due to its fast clearance. Mice injected with FITC-OVA loaded H-^{IV}Al-DMSN and DMSN showed negligible FITC signal but obvious RITC signal from nanoparticles at the injection sites after 24 h post injection, indicating fast OVA release after injection. This OVA leakage was supported by the in vitro fast release behavior of OVA from H-^{IV}Al-DMSN and DMSN in Figure S7B. FITC signal was detectable at the injection site of mice injected with OVA-FITC loaded Alhydrogel, which may be attributed to delayed OVA release from aggregated Alhydrogel. In contrast, mice injected with OVA-FITC loaded Na-^{IV}Al-DMSN displayed the most intense fluorescence of OVA-FITC than the other formulations. Additionally, OVA-FITC in Na-^{IV}Al-DMSN group was still detectable at the injection site at 48 h post injection, indicating prolonged OVA retention. One possible reason for the enhanced OVA retention is the recruitment of immune cells like neutrophils and APCs triggered by Na-^{IV}Al-DMSN at the injections site, promoting antigen uptake in accumulated immune cells after injection.

Proximal and distal LNs were extracted at 24 h and 48 h post injection, and their fluorescent signals were also determined. As shown in Figure S12B, the RITC signals from nanoparticle formulations (DMSN, Na-^{IV}Al-DMSN and H-^{IV}Al-DMSN) were stronger than that from Alhyderogel group at one day post injection, indicating the faster migration of nanoparticles to LNs, possibly due to their monodispersity and nanosize in serum containing environment compared to aggregated Alhydrogel. In the proximal LNs, the green fluorescent signals from FITC-OVA in Na-^{IV}Al-DMSN, H-^{IV}Al-DMSN and DMSN groups were also stronger than that from the Alhydrogel group at 24 h post injection. The results obtained from the distal LNs were similar with the data obtained from proximal LNs. After 48 h post injection, the only detectable FITC signal in distal LNs was from OVA-FITC loaded in Na-^{IV}Al-DMSN formulation. These data suggests that, compared to Alhydrogel which tends to aggregate into microsize after mixed with antigen (Table S1), nanosized Na-^{IV}Al-DMSN not only promote OVA transportation from the injection site to the distal LNs but also prolong the accumulation of antigen in LNs.

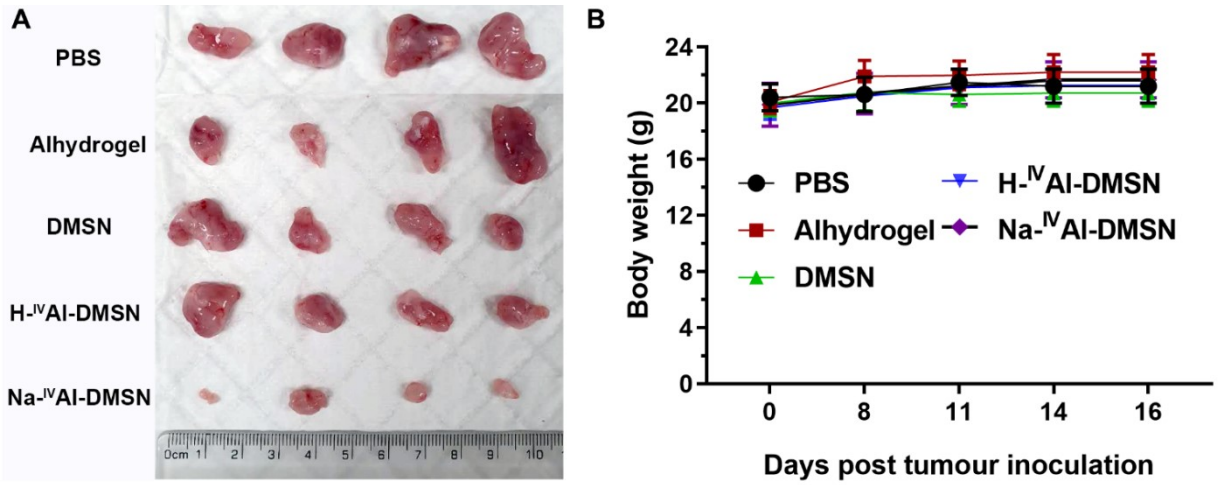

Figure S13. Tumor preventing activity of Na-^{IV}Al-DMSN on CT26 tumor. (A) Digital images of tumors collected from euthanized animals immunized by different vaccine formulations on day 16 post tumor injection. (B) The body weight changes of CT26 tumor-bearing mice during the treatment.

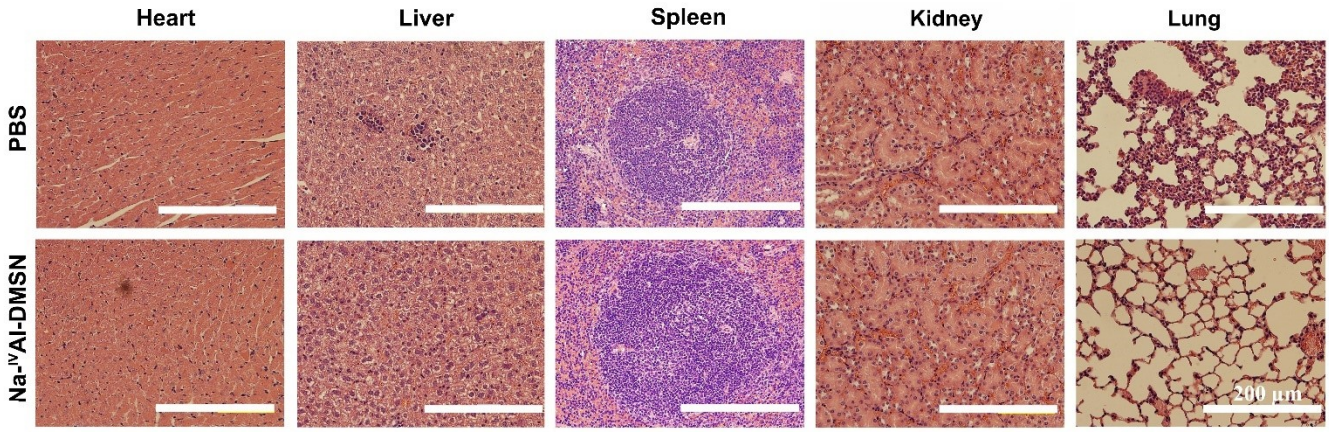

Figure S14. H&E staining of major organs (heart, liver, spleen, lung and kidney) of mice immunized with different formulations.

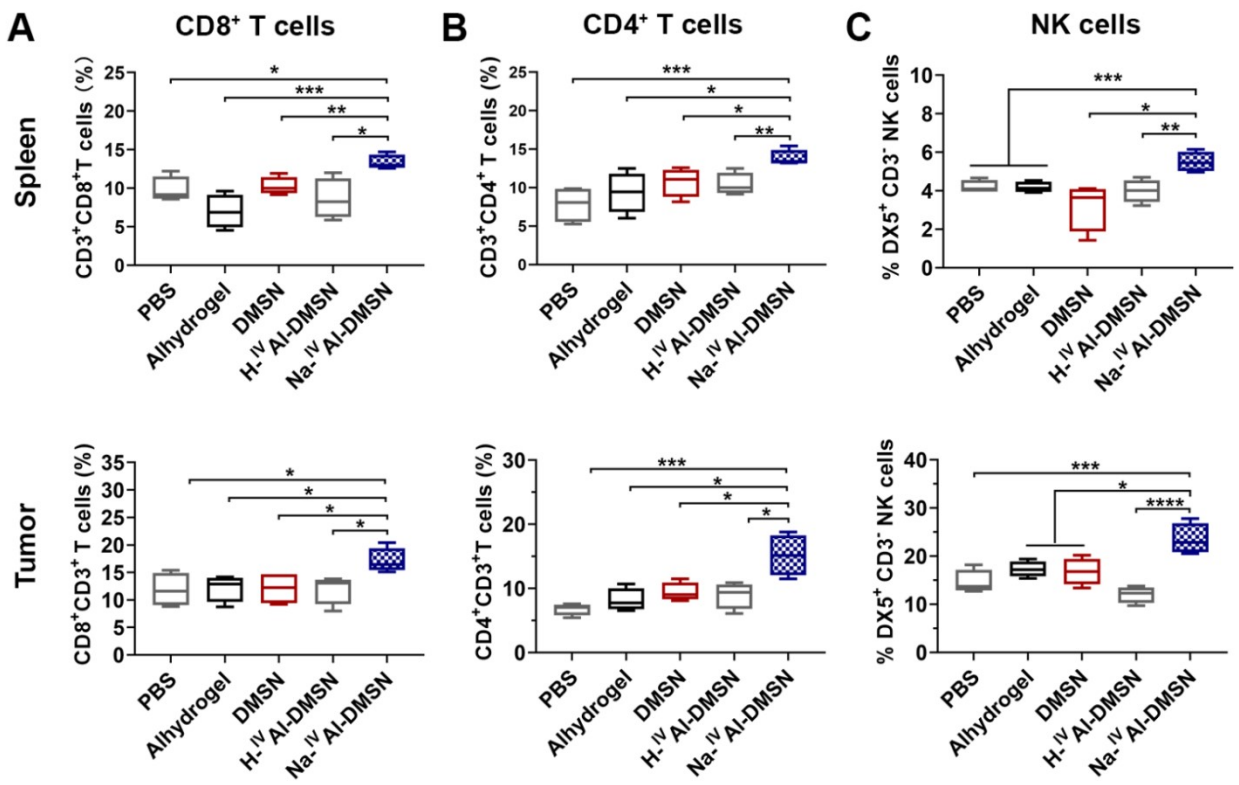

Figure S15. Flow cytometry analysis of spleenocytes profiles and tumor tissue samples including: A) $CD8^+$ T cells, B) $CD4^+$ T cells, C) NK cells. Data are presented as mean ± SD (*p<0.05, ** p <0.01, *** p <0.005).

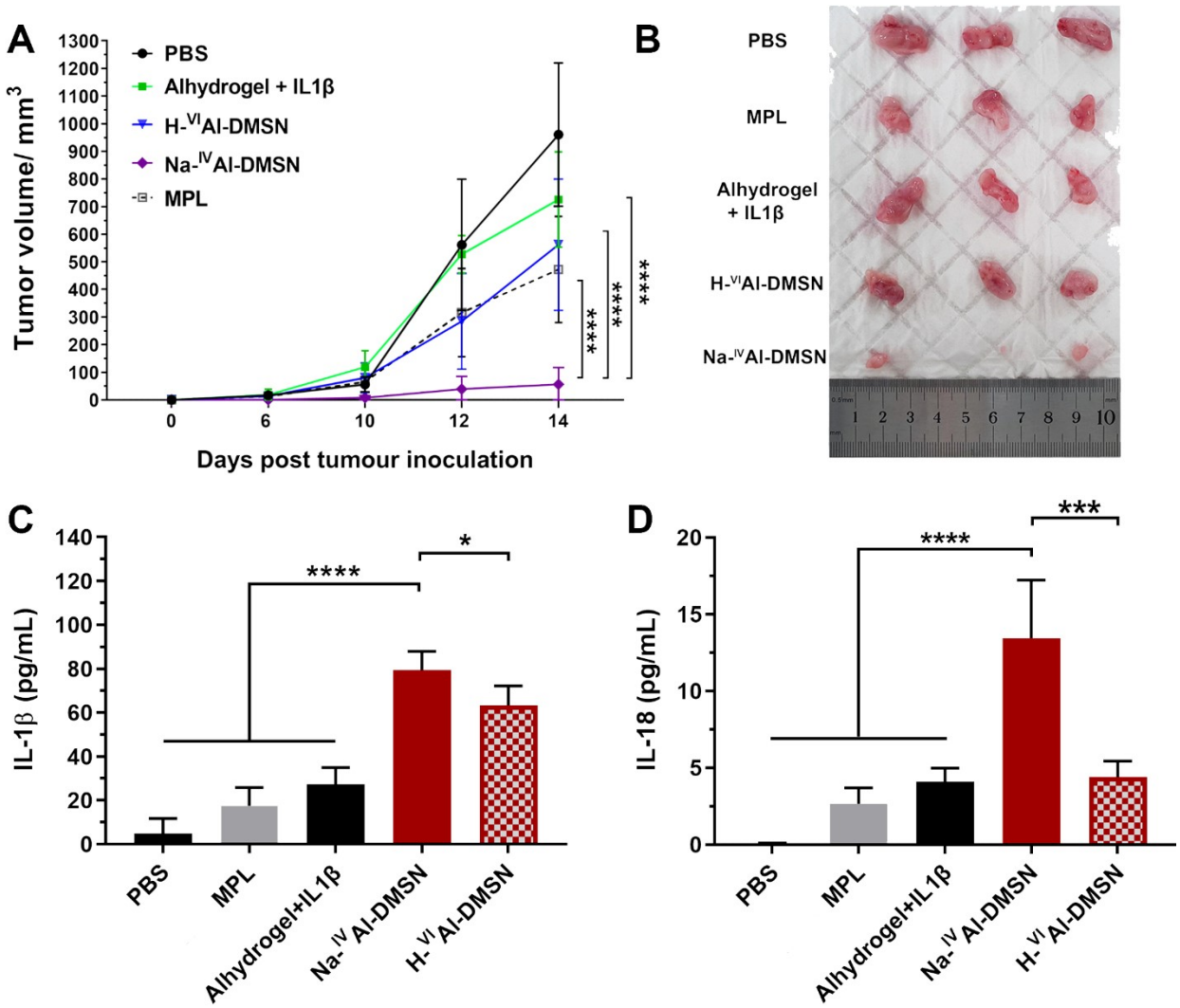

Figure S16. Na-^{IV}Al-DMSN induce anti-cancer immunity in prophylactic tumor models. CT26 cells lysates were collected and loaded with prepared nanoformulations. Balb/c mice (n = 5 per group) were immunized subcutaneously with PBS, free CT26 cell lysates with MPL (10 μg per mouse), CT26 cell lysates loaded Alhydrogel + IL-1β (0.2 μg per mouse), H-^{VI}Al-DMSN and Na-^{IV}Al-DMSN on day 0, 14, and 21. Seven days after the last immunization, the mice were challenged with 5 ×10^5 live CT26 cells in the right flank. A) Tumor growth in balb/c mice vaccinated, and tumor volume was monitored every 2 d. B) A) Digital photograph of representative tumors from PBS, MPL, Alhydrogel + IL-1β, H-^{VI}Al-DMSN and Na-^{IV}Al-DMSN. The secretion of IL-1β (C) and IL-18 (D) in sera at 14 days post tumor challenge were detected using ELISA.

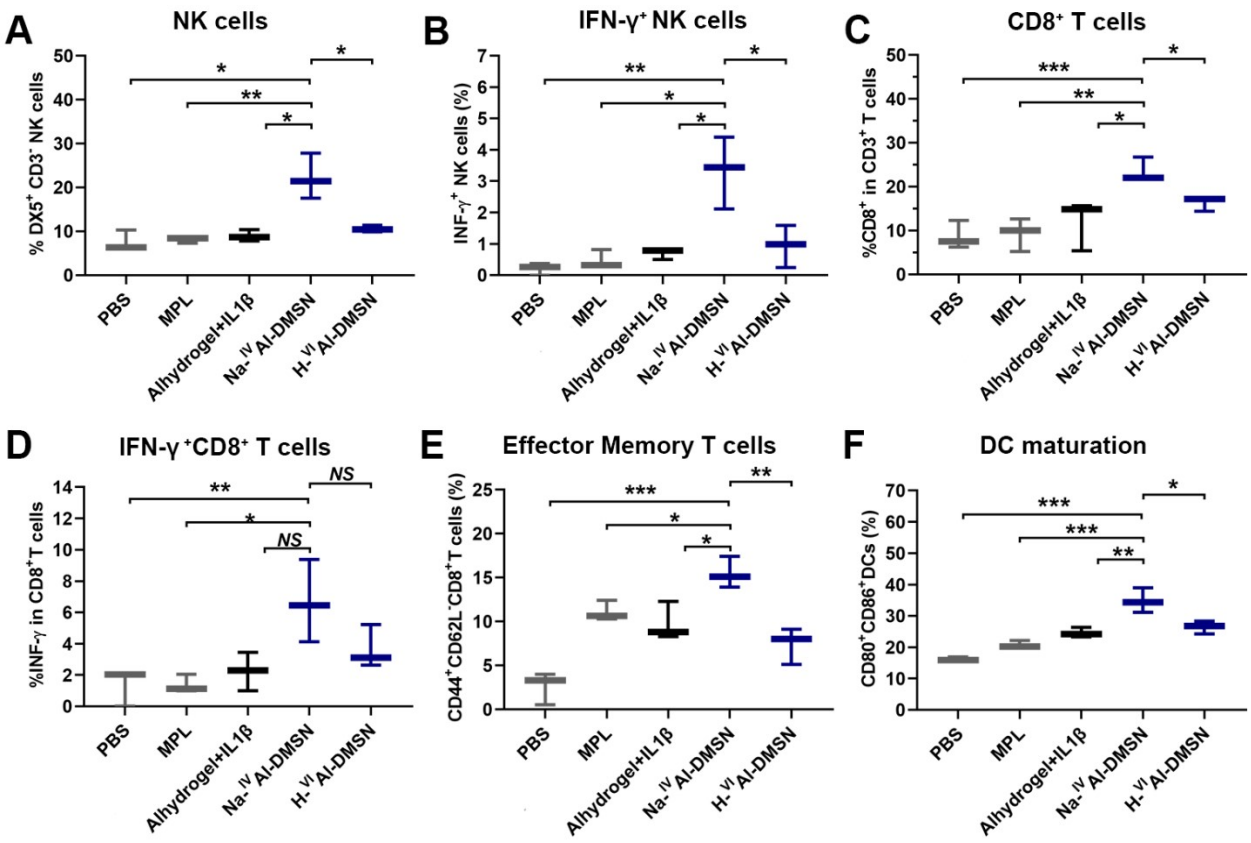

Figure S17. Flow cytometry analysis of tumor tissue samples collected on day 16 including: A) NK cells, B) IFN-γ^+ NK cells, C) $CD8^+$ T cells , D) $CD8^+$IFN-γ^+ T cells. Flow cytometry analysis of spleenocytes profiles: E) $CD44^{high}CD62L^{low}CD8^+$T cells (effector memory T cells) and F) $CD80^+CD86^+$ DCs. Data are presented as mean ± SD (*p<0.05, ** p <0.01, *** p <0.005).

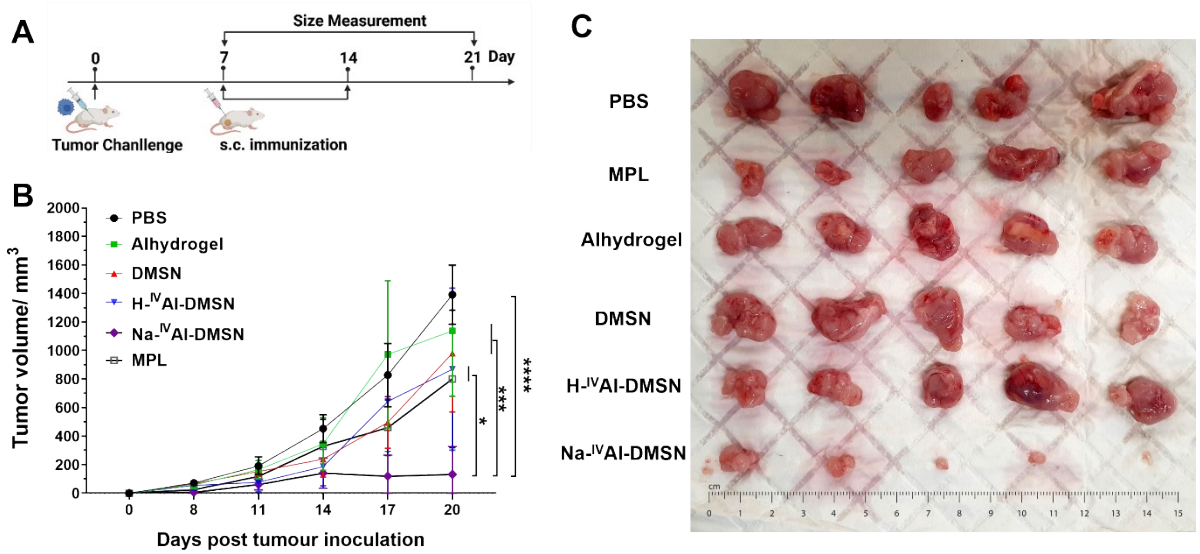

Figure S18. Na-^{IV}Al-DMSN showed antitumor activity in a therapeutic CT26 colon cancer model. A) CT26 cells lysates were collected and loaded with prepared nanoformulations. CT26 cells were subcutaneously implanted into the right flank of Balb/c mice (n = 5 per group) on day 0, and the tumors were allowed to grow for 7 d to a size of about 30-40 mm^3. The first therapeutic injection (free CT26 cell lysates, CT26 cell lysates loaded DMSN, Alhydrogel, H-^{IV}Al-DMSN and Na-^{IV}Al-DMSN) was administered on the left flank on day 7. The second injection was performed on day 14 with the same doses of CT26 cell lysates loaded formulations. B) Tumor growth in balb/c mice vaccinated, and tumor volume was monitored every 2 d. C) Digital photograph of representative tumors from PBS, MPL, Alhydrogel, DMSN, H-^{VI}Al-DMSN and Na-^{IV}Al-DMSN.

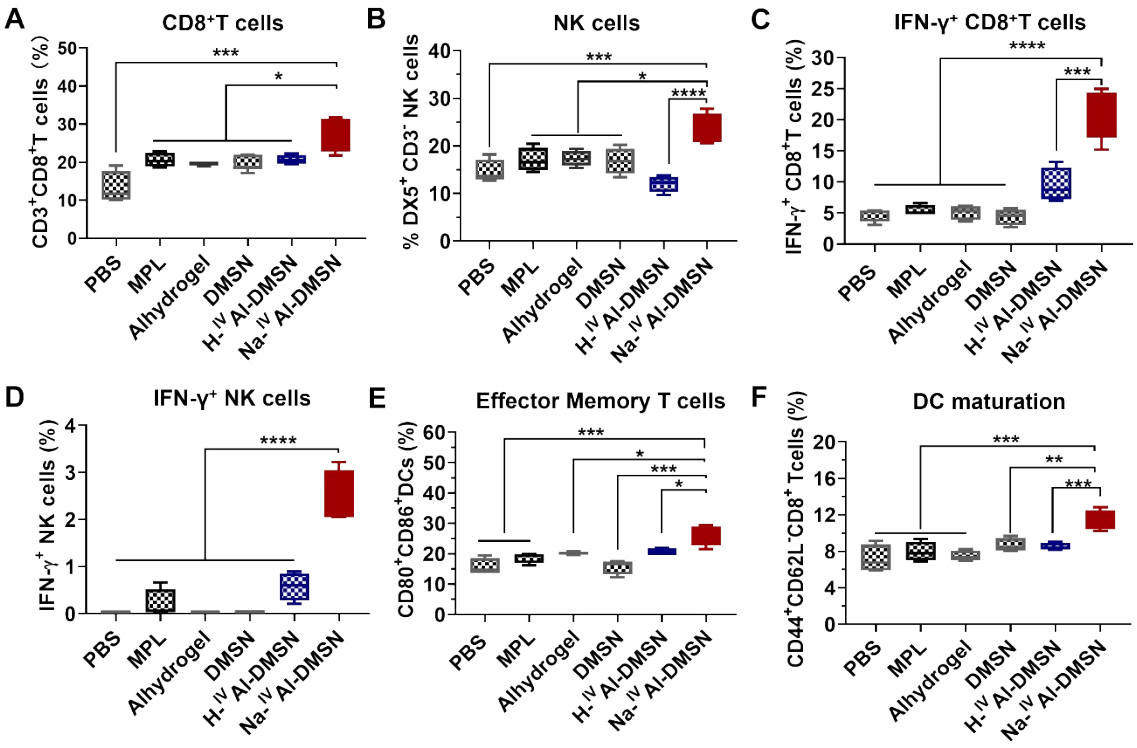

Figure S19. Flow cytometry analysis of tumor tissue samples collected on day 21 including: A) $CD8^+$ T cells, B) NK cells, C) $CD8^+$IFN-γ^+ T cells, D) IFN-γ^+ NK cells. Flow cytometry analysis of spleenocytes profiles: E) $CD44^{high}CD62L^{low}CD8^+$T cells (effector memory T cells) and F) $CD80^+CD86^+$ DCs. Data are presented as mean ± SD (*p<0.05, ** p <0.01, *** p <0.005).

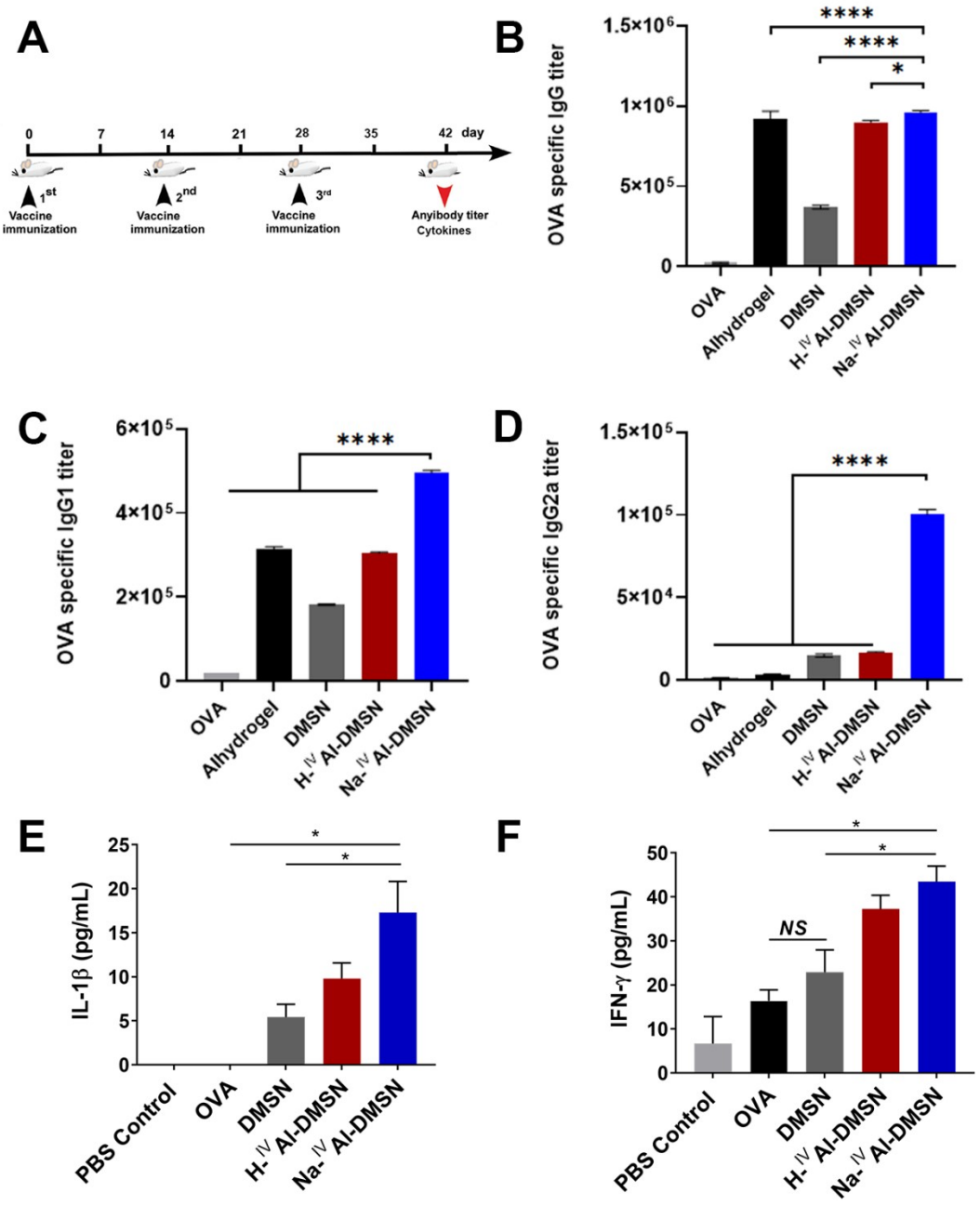

Figure S20. The effect of Na-^{IV}Al-DMSN-OVA formulations on OVA-specific antibodies production and cytokine production in vivo. A) The schematic graph of in vivo vaccination study. C57BL/6 mice were immunized with different vaccines formulations loaded with OVA as described in the text. Seven days after the third immunization, blood was withdrawn for analysis of OVA-specific antibody and cytokines production. n = 6 mice. B-D) The anti-OVA IgG (B), IgG1(C), IgG2a (D) antibody titers in sera on day 42 were detected using ELISA. E) IL-1β and F) IFN-γ in sera measured by ELISA. Bars shown are mean ±SE (n = 6), and differences between OVA and other treatments are determined using one-way ANOVA analysis. *: $p < 0.05$, **: $p < 0.01$, ***: $p < 0.001$.

As shown in Figure S20A-D, compared to soluble OVA, Na-^{IV}Al-DMSN not only dramatically enhanced the production of IgG (50-fold) but also increased the secretion of IgG1 (25-fold) and IgG2a (100-fold). More importantly, compared with the H-^{IV}Al-DMSN formulation, the Na-^{IV}Al-DMSN formulation significantly enhanced the production of anti-OVA IgG2a about by 10-fold (Figure S20D). The potent induction of these immune responses by Na-^{IV}Al-DMSN formulation could be explained by its capability to induce DC maturation and prolonging accumulation of antigen in LNs.

Table S1. Hydrodynamic size of DMSN, Na-^{IV}Al-DMSN, H-^{IV}Al-DMSN and Alhydrogel with or without OVA and dispersed in different mediums measured by DLS and PdI, their zeta potential

C[a] (s)=1 mg/mL	Hydrodynamic size (nm)						Zeta potential (mV)		
Sample	Water	PBS (pH 7.4)	PDI[b]	DMEM with 10% FBS	DMEM with 10% FBS+ OVA	PDI	Water	PBS (pH 7.4)	DMEM with 10%FBS+OVA
DMSN	226.5±2.3	246.5±4.9	0.092	258.3±1.9	292.5±7.2	0.025	-14±1.5	-12.9±4	-6.3±0.4
Na-^{IV}Al-DMSN	214.4±3.5	232.9±2.7	0.057	238.3±5.2	272.5±5.9	0.045	-30.0±1.2	-20.3±1.3	-9.5±1.2
H-^{IV}Al-DMSN	218.4±6.3	227.5±3.2	0.081	231.6±3.7	269.3±4.9	0.1	-35±2.9	-22.8±2.2	-9.8±1.6
Alhydrogel	293.1±2.6	1017±365	0.9	751.9	418.9	1	17.43±2.6	-14.4±1.6	-8.1±1.9

[a]concentration of formulations; [b] Polydispersity Index.